Supplementary Material

Methods: Chemicals

Chemical standards and solvents were purchased as follows: malonic acid (99%), 4-nitrophenol (98%), and 2,4-dinitrophenol (98%) were purchased from Acros organics. Glutaric acid (99%), oxalic acid (99.999%), benzoic acid (99%), succinic acid (99+%), pyruvic acid (98%), propionic acid (99+%), 2-methyl-4-nitrophenol (97%), maleic acid (99%), *cis*-pinonic acid (98%), and 2,4-pentanedione (99+%) were purchased from Aldrich. Inorganic salt standards (Six Cation-II and Seven Anion Standards) were purchased from Dionex and diluted. Formaldehyde (37% aqueous/methanol), sodium hydroxide pellets, potassium iodide (KI; 99.6%), iodine (100.0%), potassium hydrogen phthalate (99.95%), sodium carbonate (HPLC grade), and sodium bicarbonate (certified ACS) were purchased from Fischer. Ammonium acetate (≥99.0%), *para*-hydroxy-phenylacetic acid (POPHA; ≥98.0%), $Na_4EDTA \bullet 4H_2O$ (≥99%), CDTA (≥98%), parafuchsin (containing pararosaniline), methanesulfonic acid (MSA; ≥99.0%), acetic acid (99%), formic acid (~98%), adipic acid (≥99%), *n*-valeric acid (≥99%), azelaic acid (98%), and 4,6-dinitro-*o*-cresol (2-methyl-4,6-dinitrophenol; ≥98%) were purchased from Fluka. Salicylic acid (≥99.0%), monobasic potassium phosphate (99.99%), and catalase enzyme from bovine liver were purchased from Sigma. Buffers for pH measurement (pH 4, 7), hydrogen peroxide (30% w/w aqueous solution), and Triton X-100 non-ionic detergent were obtained from Sigma-Aldrich. Pinic acid was obtained from the Sigma-Aldrich Library of Rare Chemicals (no purity characterization was carried out). Horseradish peroxidase (Type VI, 250-330 units/mg solid using pyrogallol) was purchased from both Fisher Scientific and Sigma. Anhydrous sodium sulfite was purchased from Chempure Lab Chemicals (99.9%). Methanol and acetonitrile (LCMS grade) were purchased from Honeywell.

Stock standards of organic acids (100 mM) were prepared in water, with the exception of valeric and succinic acids, which were prepared using ~2% methanol in water. Stock standards of

nitrophenols (4 and 10 mM) were prepared using up to 40% methanol and/or 4% acetonitrile in water.

Methods: Chemical Analysis

All chemical analyses were carried out without prior filtration of the collected fog water. Most analyses were carried out using procedures previously employed for fog and cloud samples (e.g., Collett et al., 1999; Benedict et al., 2012). Information about purchased chemicals can be found in the Supporting Information. S(IV), which includes dissolved sulfur dioxide, bisulfite, sulfite, and hydroxymethanesulfonate (HMS), was measured after reaction with 4,4'-[(4-Imino-2,5-cyclohexadien-1-ylidene)methylene]dianiline (pararosaniline) via UV/visible absorption spectrometry (Shimadzu UV-1800 spectrophotometer) at 580 nm according to a modified procedure introduced by Dasgupta et al. (1980; 1981). Formaldehyde was reacted with 2,4-pentanedione and ammonia to form diacetyldihydrolutidine (DDL), which can be measured via fluorescence spectrometry at an excitation wavelength of 412 nm and an emission wavelength of 510 nm (Labteq fluorescence plate reader) following a procedure published by Dong and Dasgupta (1987). Formaldehyde naturally complexed in the form of HMS is included in the quantified formaldehyde using this method. The mean of three replicate formaldehyde measurements was used for each sample. Total peroxides (organic peroxides and hydrogen peroxide) were reacted with *para*-hydroxy-phenyl-acetic acid (POPHA) to form a fluorescent dimer in the presence of horseradish peroxidase (412 nm excitation, 510 nm emission; Labteq fluorescence plate reader; Lazrus et al., 1986). A solution of triiodide (I_3^- from KI/I_2) was used to calibrate the stock solution of hydrogen peroxide. The mean of three replicate peroxides measurements was used for each sample. TOC was measured using a Sievers Model 800 Turbo TOC Analyzer in Turbo mode (via digestion of carbonaceous material to CO_2 followed by conductivity detection). Major inorganic ions were quantified using a Dionex DX-500 ion chromatography (IC) system with conductivity detection; cations were separated along a Dionex

CS12A analytical column with an installed CG12 guard column and CSRS ULTRA II suppressor using MSA as eluent; anions were separated along a Dionex AS14A analytical column with an installed AG14A guard column and ASRS ULTRA II suppressor using CO_3^{-2}/HCO_3^- eluent. Organic acids were analyzed using a gradient Dionex IC system with a Dionex AS11-HC analytical column, AG11 guard column, and ASRS ULTRA II suppressor using NaOH eluent and a conductivity detector. A small number of samples were also analyzed after separation using (-)-ESI-HR-ToF-MS to confirm the identifications of eluted organic acids. Additional organic molecules were identified via HPLC-(-)-ESI-HR-ToF-MS: a Kinetex 2.6 μm particle size XB-C18 column designed for polar organic species separation with 100 Å pore size and 3.00 mm internal diameter was used to separate organic species (higher molecular mass organic acids, phenols and organosulfates) via a 0.1% formic acid/methanol gradient elution. The HPLC-(-)-ESI-HR-ToF-MS system consisted of an Agilent 1100 Series LC with Agilent MSD/ToF detector. Agilent EI-TOF tuning mix was used to perform external mass calibration prior to analyses, initially giving ±1 ppm mass accuracy. Mass accuracies during analysis are tabulated in Table 2, and are typically <15 ppm. External calibrations performed on the HPLC-(-)-ESI-HR-ToF-MS were linear ($r^2 > 0.90$). Mass spectral results were filtered so that only species with abundances ≥ 500 abundance units (a.u.) were included. A mass range of 100 to 300 Da was chosen for inclusion in the analyses of these species to exclude organic species identified via IC (organic acids) and compounds with uncertain formula assignments at higher masses.

Methods: Statistical Calculations

Limits of detection (LODs) were estimated from blanks collected after each event during the sampling campaign, and calculated as $ts\sqrt{((N_s+N_{blk})/(N_s*N_{blk}))}$ where N_{blk} is the number of replicate blanks, N_s is the number of replicate samples, t is the Student's t-statistic value for the given N_{blk} at the one-tailed 95% confidence level, and s is the standard deviation of the replicate blanks. Uncertainties were calculated as $ts/\sqrt{N_s}$ for replicate standard solutions at a median

concentration from each calibration curve, where N is the number of standard replicates (≥ 3), t is the Student's t-statistic value for the given N at the two-tailed 95% confidence level, and s is the standard deviation of the standard replicates.

Results: Changes in Composition during Fog Events

Constraining the processes leading to composition changes during a fog event is difficult. Trends in concentrations of major ions are shown in Fig. SI-4 for two fog events through which multiple fog water samples were collected (2 and18 July). Although clearly demonstrating that AAOP reactions occurred during these events is not possible, there are changes during the fog events that are apparent within the measured chemical and physical parameters. During the dissipation stage of fogs observed on 2 and 18 July, the LWC decreased and concentrations of all species measured increased. While LWC and constituent concentrations have a generally inverse relationship during the events, the LWC explains 25% or less of concentration variation ($r^2 \leq 0.25$) in samples overall for small and large samples. On 18 July (Fig. SI-4, right), the decrease in the magnitude of concentrations at 7:30 am agrees with previously observed depositional velocities for individual inorganic species (Herckes et al., 2007). Throughout the two fog events, changes in total low molecular mass organic acid concentrations, which might reflect oxidation of organic species within the fog water, are either low or follow trends of other inorganic species, consistent with a dominance of physical processes. The lack of clear evidence for supporting or negating aqueous organic reactions within these specific fog events emphasizes the utility of laboratory studies in which many chemical and physical variables can be controlled.

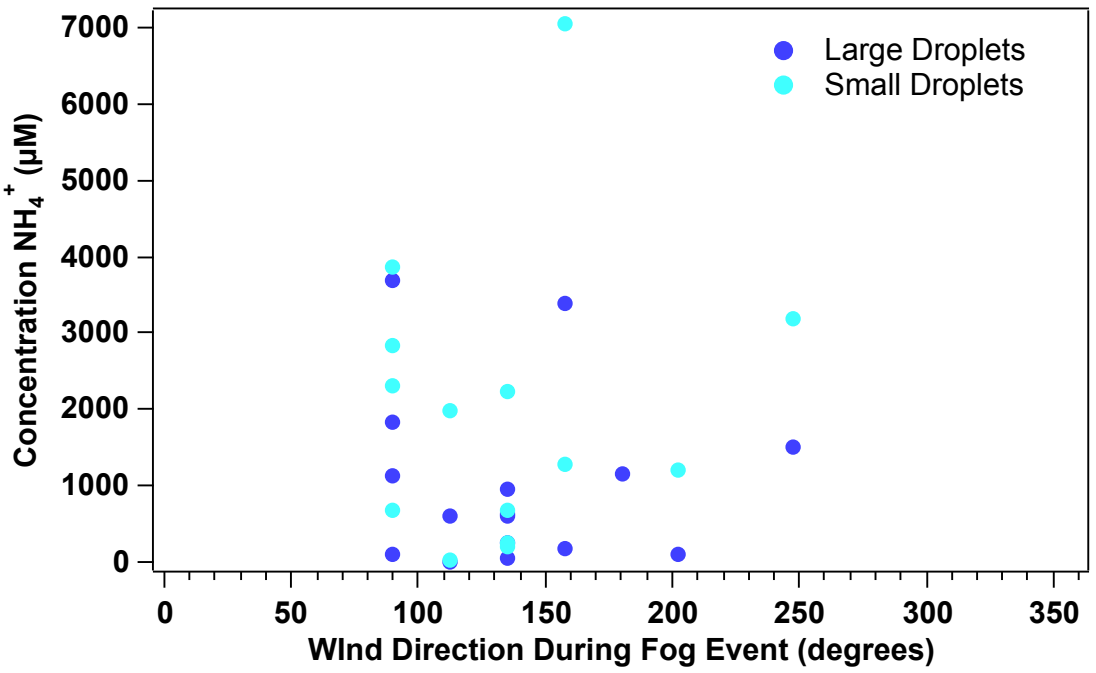

97

98

99 **Figure SI-1.** Ammonium concentrations during fog events as a function of wind directions

100 measured at co-located meteorological station. No correlation can be observed between NH_4^+ and

101 wind, showing that the source of this species was likely long-rang transport as NH_4NO_3.

102

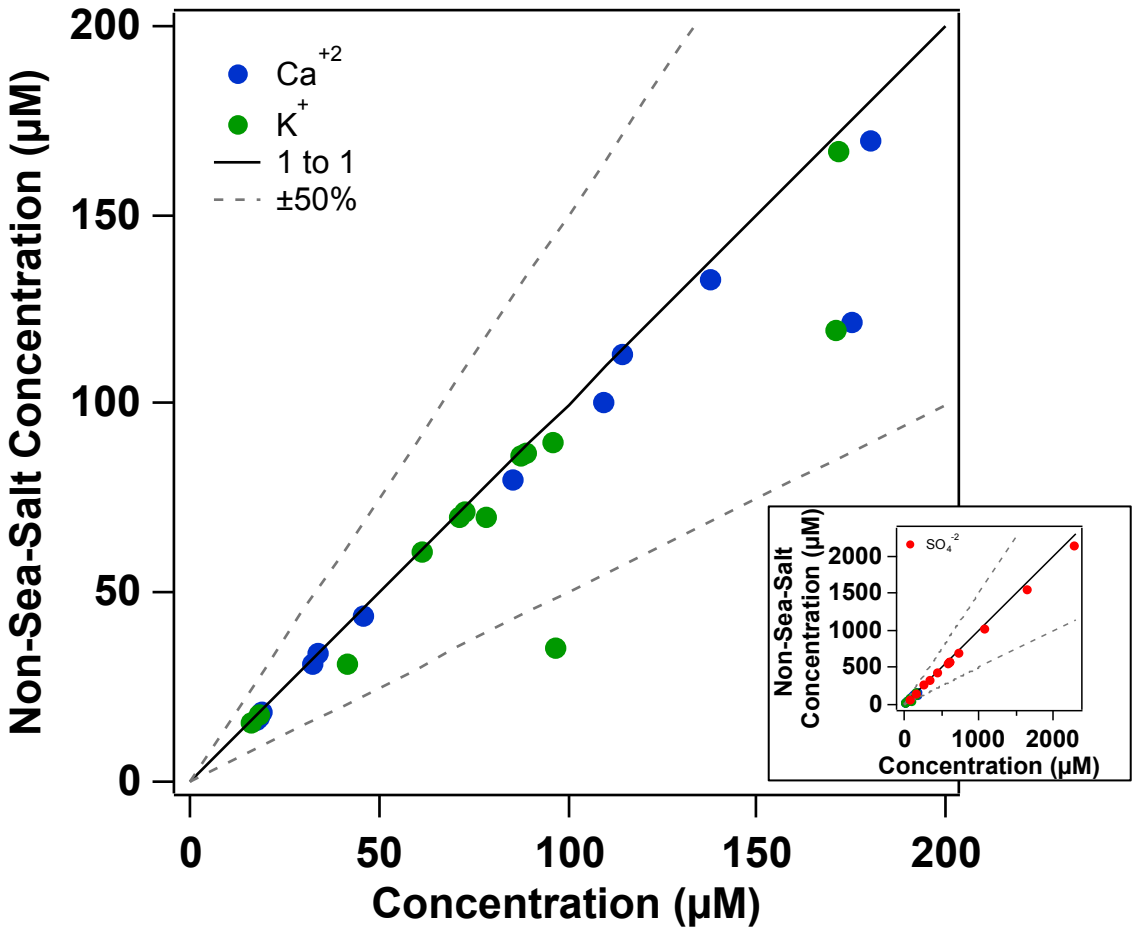

103

104 **Figure SI-2.** nss components of several ionic species, calculated using molar ratios of species and

105 Na^+ in sea salt. Area between solid line denoting 100% nss contribution and dashed line denoting

106 50% below includes most data points. Inset shows nss-SO_4^{-2} contribution. nss-Cl^- concentrations

107 are sometimes well below zero (due to Cl^- depletion) and are therefore not shown.

108

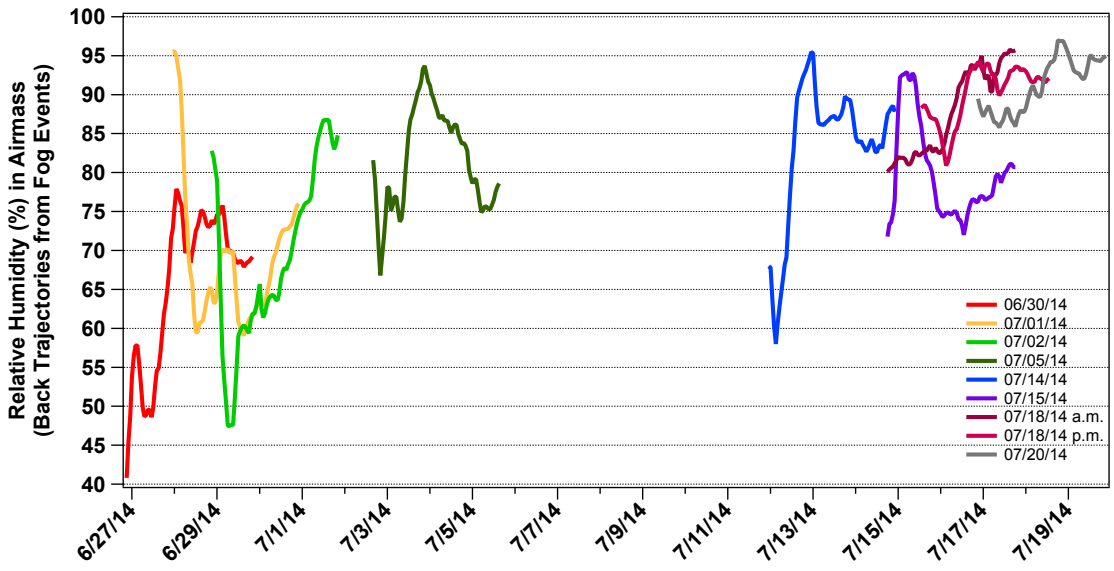

109

110 **Figure SI-3.** Relative humidity outputted from HySPLIT back trajectories initialized at the
111 beginning of each fog event sampled in this study. All samples with the exception of that
112 collected on 30 June were impacted by air masses that had been at high RH (>80%) for a portion
113 of the previous 72 hours.

114

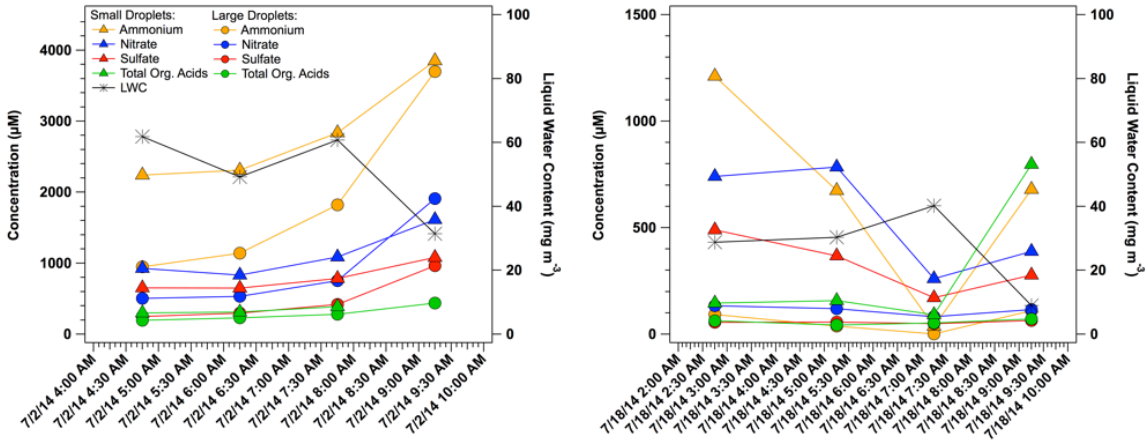

115

Figure SI-4. Chemical trends with time for two fog events during which multiple fog water samples were collected (on the mornings of 2 and 18 July 2014). LWC was calculated as the mean value measured by the PVM through the duration of each fog sample (times along the bottom of the plot are at the start of each sampling period).